Research Article

Mst. Razia Pervin, Harun-Or-Roshid*, Alrazi Abdeljabbar*, Pinakee Dey, and Shewli Shamim Shanta

Dynamical structures of wave front to the fractional generalized equal width-Burgers model *via* two analytic schemes: Effects of parameters and fractionality

https://doi.org/10.1515/nleng-2022-0328
received July 25, 2023; accepted September 8, 2023

Abstract: This work focuses on the fractional general equal width-Burger model, which describes one-dimensional wave transmission in nonlinear Kerr media with combined dispersive and dissipative effects. The unified and a novel form of the modified Kudryashov approaches are employed in this study to investigate various analytical wave solutions of the model, considering different powers of nonlinearity in the Kerr media. As a result, a wide range of structural solutions, including trigonometric, hyperbolic, rational, and logarithmic functions, are formulated. The achieved solutions present a kink wave, a collision of kink and periodic peaked soliton, exponentially increasing wave profiles, and shock with a dark peaked wave. The obtained solutions are numerically demonstrated for specific parameter values and general parametric powers of nonlinearity. We analyzed the effect of existing parameters on the obtained wave solutions with numerical graphics. Moreover, the stability of the model is analyzed with a perturbed system. Furthermore, a comparison with published results in the literature is provided, highlighting the differences and similarities. The achieved results showcase the diversity of structural solutions obtained through the proposed approaches.

Keywords: fractional GEW-Burger model, Jumarie's Riemann–Liouville derivative, unified scheme, Kerr media, dispersive effects, dissipative effects.

*** Corresponding author: Harun-Or-Roshid,** Department of Mathematics, Pabna University of Science and Technology, Pabna-6600, Bangladesh, e-mail: harunorroshidmd@gmail.com
*** Corresponding author: Alrazi Abdeljabbar,** Department of Mathematics, Khalifa University, Abu Dhabi, P O Box 127788, United Arab Emirates, e-mail: raziahelal@yahoo.com
Mst. Razia Pervin: Department of Mathematics, Mawlana Bhashani Science and Technology University, Tangail, Bangladesh; Department of Mathematics, University of Rajshahi, Rajshahi-6205, Bangladesh
Pinakee Dey: Department of Mathematics, Mawlana Bhashani Science and Technology University, Tangail, Bangladesh
Shewli Shamim Shanta: Department of Mathematics, University of Rajshahi, Rajshahi-6205, Bangladesh

1 Introduction

Nonlinear fractional evolution models have emerged as powerful tools for modeling various phenomena in science and engineering, particularly in the context of miniature, sensitive, and microscopic systems [1–3]. These models have found applications in capturing complex physical states [4–6] and are instrumental in accurate modeling of intricate nonlinear phenomena. In the existing literature, different types of fractional models have been proposed to facilitate precise modeling. Examples include the Jumarie Riemann–Liouville (JRL) fractional model [7,8], modified Riemann–Liouville fractional model [9,10], conformable time-fractional model [11,12], fractional beta model [13,14], M-fractional model [15], and many others. Among these fractional models, the JRL fractional model satisfies most of the desirable properties of differentiation, while other models may exhibit some undesirable or anomalous behaviors. In light of this, the present write-up focuses on the spatial-temporal fractional general equal width (GEW)-Burgers model in the framework of the JRL fractional sense. The model is represented as follows:

$$D_t^{\beta}E + \ell D_x^{\alpha}E^{n+1} - rD_{xx}^{2\alpha}E - kD_{xxt}^{2\alpha,\beta}E = 0, \quad n > 1, \tag{1}$$

where D^{α} and D^{β} denote the JRL fractional derivatives, and α, β, and m are real constant parameters. The GEW-Burgers model incorporates fractional order derivatives with respect to both space and time variables, and the novel fractional JRL derivative is employed for precise characterization.

Only a limited number of researchers have investigated the GEW-Burgers equation using analytical techniques. Nuruddeen and Nass [15] employed the Kudryashov technique to extract exact solitary wave solutions for both

the classical and fractional derivative versions of the model. Hamdi *et al.* [16] derived a few exact results for the model using only the classical derivative. Research on this model is scarce, yet it holds significant applications in wave transmission within nonlinear media, encompassing both dispersive and dissipative effects. Notably, GEW-Burger has been studied solely in the context of the conformable fractional case [15].

This research aims to modify the model into the form given in Eq. (1) using the JRL fractional sense. The key question now pertains to identifying appropriate techniques for exploring the intricate dynamics arising from integrating our proposed fractional nonlinear model (1). Various techniques have been employed in recent works to obtain exact solutions for fractional partial differential equations, ranging from semi-analytical schemes to unified procedures [17–34]. Among them, the unified technique stands out due to its incorporation of tanh and exp-functions approaches.

In this write-up, we shed light on the use of the Unified method [32–34] to analytically investigate the fractional GEW-Burgers model. In addition, a novel form of the modified Kudryashov (NFMK) [35] scheme enables the discovery of innovative arbitrary number base wave solutions.

The structure of this write-up is as follows: Section 2 provides elementary definitions and properties of JRL fractional derivatives. Integral techniques are briefly explained in Section 3. In Section 4, we extract novel solutions of the space-time fractional generalised equal width-Burgers model using the unified and NFMK techniques. The results are presented in Section 5, followed by a comparison with other results in Section 6. Finally, the write-up concludes with a summary in Section 7.

2 Properties of JRL derivative

In this section, we compile essential properties and notes related to the definition of β-order fractional differentiation [8] for a continuous function denoted by $\psi : \Re \to \Re$.

The β-order fractional differentiation of a continuous function is represented as follows:

$$D^{\beta}\psi(x) = \begin{cases} \dfrac{1}{\Gamma(1-\beta)}\dfrac{\mathrm{d}}{\mathrm{d}x}\displaystyle\int_0^x (x-t)^{-\beta}(\psi(t)-\psi(0))\mathrm{d}t, \\ 0 < \beta < 1 \\ (\psi^{(n)}(x))^{(\beta-n)}, \quad n \le \beta < n+1, \quad n \ge 1, \end{cases} \tag{2}$$

where $\Gamma(x)$ is indicated as $\Gamma(x) = \int_0^{\infty} e^{-t}t^{x-1}\mathrm{d}x$.

Some significant properties are as follows:

(i) $D_x^{\beta}x^p = \frac{\Gamma(1+p)}{\Gamma(1+p-\beta)}x^{p-\beta}$.

(ii) $D_x^{\beta}(q\psi(x) + r\phi(x)) = qD_x^{\beta}(\psi(x)) + rD_x^{\beta}(\phi(x))$, q, r are constants.

(iii) $D_x^{\beta}\psi(\chi) \overset{\chi=\phi(x)}{=} \frac{d\psi}{d\chi}D_x\psi$.

For others properties see [8].

3 Methodology

This segment represents fractional unified and NFMK schemes as well as their applications to the space–time JRL fractional GEW–Burger model to accomplish new solutions.

3.1 Basic information of fractional unified scheme

This section illustrates fractional unified scheme [32–34] for guiding analytical solutions to nonlinear fractional evolution equations (NFEEs) in a succeeding manner. Consider an NFEE in independent variables x and t, which is specified by

$$H(q,\ D_x^{\alpha}q,\ D_{xxt}^{2\alpha,\beta}q,\ D_{xxx}^{3\alpha}q,\ D_t^{\beta}q,\ D_{tt}^{2\beta}q, \ldots) = 0, \tag{3}$$

where $q(x,\ t)$ is indefinite function, H is polynomial of $q = q(x, t)$ accomplished with its derivatives.

Step 1: Converting the NFEE into ordinary differential equation (ODE) with the advantages of operating wave mapping

$$q(x,t) = \upsilon(\eta), \quad \eta = \frac{kx^{\alpha}}{\sqrt{1+\alpha}} - w\frac{t^{\beta}}{\sqrt{1+\beta}}, \tag{4}$$

where k and ω are the wave number and velocity, respectively. By shifting Eq. (4) into Eq. (3), an ODE can be achieved, *i.e.*,

$$P(\upsilon_{\eta},\ \upsilon_{\eta\eta},\ \upsilon_{\eta\eta\eta},\ \upsilon\upsilon_{\eta},\ \upsilon_{\eta\eta\eta}, \ldots) = 0. \tag{5}$$

Step 2: Now Eq. (5) can be integrated requisite times with integral constant as zero.

Consider that Eq. (5) has a series solution as follows:

$$\upsilon(\eta) = L_0 + \sum_{i=1}^{N}[L_iS(\eta)^i + M_iS(\eta)^{-i}], \tag{6}$$

where L_i and M_i ($i = 0,\ 1, \ldots\ N$) are constants to be evaluated afterward. We also should treat that L_N and M_N both could not be zero together. The Riccati equation can be elated by the function $S(\eta)$,

$$S' = (S(\eta))^2 + \lambda, \tag{7}$$

which has results as:

Case 1: On condition $\lambda < 0$, yields hyperbolic results:

$$S(\eta) = \begin{cases} \dfrac{\sqrt{-(a^2+b^2)\lambda} - a\sqrt{-\lambda}\cosh(2\sqrt{-\lambda}(\eta+c))}{a\sinh(2\sqrt{-\lambda}(\eta+c))+b}, \\ \dfrac{-\sqrt{-(a^2+b^2)\lambda} - a\sqrt{-\lambda}\cosh(2\sqrt{-\lambda}(\eta+c))}{a\sinh(2\sqrt{-\lambda}(\eta+c))+b}, \\ \dfrac{\sqrt{-\lambda}\{\cosh(2\sqrt{-\lambda}(\eta+c)) - \sinh(2\sqrt{-\lambda}(\eta+c)) - a\}}{a+\cosh(2\sqrt{-\lambda}(\eta+c)) - \sinh(2\sqrt{-\lambda}(\eta+c))}, \\ \dfrac{\sqrt{-\lambda}\{a - \cosh(2\sqrt{-\lambda}(\eta+c)) - \sinh(2\sqrt{-\lambda}(\eta+c))\}}{a+\cosh(2\sqrt{-\lambda}(\eta+c)) + \sinh(2\sqrt{-\lambda}(\eta+c))}, \end{cases} \tag{8}$$

Case 2: On $\lambda > 0$, yields trigonometric solution:

$$S(\eta) = \begin{cases} \dfrac{\sqrt{(a^2-b^2)\lambda} - a\sqrt{\lambda}\cos(2\sqrt{\lambda}(\eta+c))}{a\sin(2\sqrt{\lambda}(\eta+c))+b}, \\ \dfrac{-\sqrt{(a^2-b^2)\lambda} - a\sqrt{\lambda}\cos(2\sqrt{\lambda}(\eta+c))}{a\sin(2\sqrt{\lambda}(\eta+c))+b}, \\ \dfrac{\sqrt{\lambda}\{i\cos(2\sqrt{\lambda}(\eta+c)) + \sin(2\sqrt{\lambda}(\eta+c)) - ia\}}{a+\cos(2\sqrt{\lambda}(\eta+c)) - i\sin(2\sqrt{\lambda}(\eta+c))}, \\ \dfrac{\sqrt{\lambda}\{-i\cos(2\sqrt{\lambda}(\eta+c)) + \sin(2\sqrt{\lambda}(\eta+c)) + ia\}}{a+\cos(2\sqrt{\lambda}(\eta+c)) + i\sin(2\sqrt{\lambda}(\eta+c))}, \end{cases} \tag{9}$$

where $a \neq 0$ and b, c are free invariable.

Case 3: On $\lambda = 0$, yields rational solution:

$$S(\eta) = -\frac{1}{\eta + c}. \tag{10}$$

Step 3: Using Eq. (7), the value of N in Eq. (5) can be underscored by incorporating Eq. (6) into Eq. (5) through the homogeneous balance principle. We extract coefficients of same power of $S(\eta)$ from both sides, produces a set of constraints. Solving the set for L_i, M_i $(i = 0, 1, \ldots, N)$, k, and ω and putting these into Eq. (6) with solutions of Eq. (7) yields solutions of Eq. (3).

3.2 Basic phases of NFMK technique

The trial result of Eq. (5) in the ensuing form is

$$\upsilon(\eta) = \sum \mu_i \psi^i(\eta), \tag{11}$$

where μ_i $(i = 0, 1, \ldots, m)$ are invariables and deliberated afterward. Evaluating equilibrium number $\psi(\eta)$ can be recognized as follows:

$$\psi(\eta) = \frac{p\Theta(\eta)}{p + g(\Theta(\eta) - 1)}, \; g \neq 0, \tag{12}$$

where p and r are calculative constants that are achieved later and the function obliges the indicated differential model as follows:

$$\frac{\mathrm{d}\Theta(\eta)}{\mathrm{d}\eta} = \delta \log(a)(\Theta(\eta) - 1)\Theta(\eta). \tag{13}$$

To develop unknown constants, Eq. (11) into Eq. (4) combining use of Eqs (12) and (13). Formerly, transform to a polynomial of $\Theta^i(\eta)$ and cautious unknown coefficients of perfectly $\Theta^i(\eta)$ are equating as zero, yielding a class of equations. Thus, the obtained structures are resolved *via* maple-18, which completed the desired unfamiliar parameters as well as the results of the model (4).

The integrated result of Eq. (13) is

$$\Theta(\eta) = \frac{1}{1 + ca^{\delta\eta}}. \tag{14}$$

Remark: Our new modified Kudryashov's (MK) technique familiarized result in terms of a series $\psi(\eta) = \frac{p\Theta(\eta)}{p + r(\Theta(\eta)-1)}$; $r \neq 0$ with $\Theta(\eta) = \frac{1}{1+ca^{\delta\eta}}$, *i.e.*, numbers base wave variable, which provides a new category of wave outlines in the studied arena, whereas MK's structure (Hosseini *et al.* [12]) used $\varphi(\xi) = \frac{1}{1+da^{\xi}}$.

4 Integrate the fGEW-Burgers model to extraction solutions

Recall space–time JRL fractional GEW-Burgers model (Eq. (1)) as well as assembling the wave transformation

$$E(x, t) = E(\eta), \quad \eta = \frac{x^{\alpha}}{\sqrt{1+\alpha}} - w\frac{t^{\beta}}{\sqrt{1+\beta}}.$$

Eq. (1) turned to an ODE,

$$-wE' + \ell(E^{n+1})' - rE'' + wkE''' = 0. \tag{15}$$

By integrating Eq. (15) once, as well as bearing in mind integral constant as zero, attains

$$-wE + \ell(E^{n+1}) - rE' + wkE'' = 0. \tag{16}$$

Evaluating balance from highest derivatives with the nonlinear term $(E^{n+1}, \; E'')$ in Eq. (15) yields $N = \frac{2}{n}$.

Incorporating the mapping $E = \upsilon^{2/n}$, Eq. (16) switches to

$$\begin{aligned} -wn^2\upsilon^2 + n^2\ell\upsilon^4 - 2nr\upsilon\upsilon' + (4wk - 2wnk)\upsilon'^2 \\ + 2wnk\upsilon\upsilon'' = 0. \end{aligned} \tag{17}$$

The next sub-steps are going to exploit wave solutions through the fractional unified and NFMK techniques.

4.1 Solutions by fractional unified technique

Balancing the highest derivatives and nonlinear term (*i.e.*, $\upsilon^4, \; \upsilon\upsilon''$) in Eq. (17), one can achieve $N = 1$, which refers to using in Eq. (6) that

$$\upsilon(\eta) = L_0 + L_1 S(\eta) + \frac{M_1}{S(\eta)}. \tag{18}$$

The following algebraic equations, by replacing Eq. (18) into Eq. (17) as well as putting every coefficient of $S(\eta)$ to zero, yields

$$\begin{aligned}
&2knw\lambda^2 M_1^2 + \ell n^2 M_1^4 + 4kw\lambda^2 M_1^2 = 0,\\
&4knw\lambda^2 L_0 M_1 + 4\ell n^2 L_0 M_1^3 + 2nr\lambda M_1^2 = 0,\\
&8knw\lambda^2 L_1 M_1 + 6\ell n^2 L_0^2 M_1^2 + 4\ell n^2 L_1 M_1^3 - 8kw\lambda^2 L_1 M_1\\
&+ 8kw\lambda M_1^2 - n^2 w M_1^2 + 2nr\lambda L_0 M_1 = 0,\\
&4\ell n^2 L_0^3 M_1 + 12\ell n^2 L_0 L_1 M_1^2 + 4knw\lambda L_0 M_1 - 2n^2 w L_0 M_1 + 2nr M_1^2 = 0,\\
&-2knw\lambda^2 L_1^2 + \ell n^2 L_0^4 + 12\ell n^2 L_0^2 L_1 M_1 + 6\ell n^2 L_1^2 M_1^2 + 16knw\lambda L_1 M_1\\
&+ 4kw\lambda^2 L_1^2 - 2knw M_1^2 - 16kw\lambda L_1 M_1 - n^2 w L_0^2 - 2n^2 w L_1 M_1\\
&- 2nr\lambda L_0 L_1 + 4kw M_1^2 + 2nr L_0 M_1 = 0,\\
&4\ell n^2 L_0^3 L_1 + 12\ell n^2 L_0 L_1^2 M_1 + 4knw\lambda L_0 L_1 - 2n^2 w L_0 L_1 - 2nr\lambda L_1^2 = 0,\\
&6\ell n^2 L_0^2 L_1^2 + 4\ell n^2 L_1^3 M_1 + 8knw L_1 M_1 + 8kw\lambda L_1^2 - n^2 w L_1^2 - 8kw L_1 M_1 - 2nr L_0 L_1 = 0,\\
&4\ell n^2 L_0 L_1^3 + 4knw L_0 L_1 - 2nr L_1^2 = 0,\\
&\ell n^2 L_1^4 + 2knw L_1^2 + 4kw L_1^2 = 0.
\end{aligned} \tag{19}$$

Solving the above systems of Eq. (19), one obtains the succeeding results:

Set 1:

$$n = 4(\lambda k + \sqrt{\lambda^2 k^2 + \lambda k}), \quad w = \pm\frac{r}{2\sqrt{-\lambda k^2 - k}}, \quad L_0 = \pm\frac{1}{2^{3/2}}\sqrt{\frac{r}{\ell\sqrt{-\lambda k^2 - k}}},$$
$$L_1 = \pm\frac{1}{2^{3/2}}\frac{1}{\lambda}\sqrt{\frac{\lambda^2 k^2 + \lambda k}{-\lambda k^2 - k}}\sqrt{\frac{r}{\ell\sqrt{-\lambda k^2 - k}}}, \quad M_1 = 0.$$

The following general solutions of Eq. (1) can be found by **Set 1** and combining Eqs (8), (9), (10), and (18):

For $\lambda < 0$,

$$E_{1,2} = \left[L_0\left\{1 + \frac{\sqrt{\lambda^2 k^2 + \lambda k}}{\lambda\sqrt{-\lambda k^2 - k}}\frac{\sqrt{-(a^2+b^2)\lambda} - a\sqrt{-\lambda}\,\cosh(2\sqrt{-\lambda}(\eta+c))}{a\sinh(2\sqrt{-\lambda}(\eta+c)) + b}\right\}\right]^{\frac{1}{2(\lambda k+\sqrt{\lambda^2 k^2+\lambda k})}},$$

$$E_{3,4} = \left[L_0\left\{1 - \frac{\sqrt{\lambda^2 k^2 + \lambda k}}{\lambda\sqrt{-\lambda k^2 - k}}\frac{\sqrt{-(a^2+b^2)\lambda} + a\sqrt{-\lambda}\,\cosh(2\sqrt{-\lambda}(\eta+c))}{a\sinh(2\sqrt{-\lambda}(\eta+c)) + b}\right\}\right]^{\frac{1}{2(\lambda k+\sqrt{\lambda^2 k^2+\lambda k})}},$$

$$E_{5,6} = \left[\pm L_0\left\{1 + \frac{\sqrt{\lambda^2 k^2 + \lambda k}}{\lambda\sqrt{-\lambda k^2 - k}}\frac{\sqrt{-\lambda}\{\cosh(2\sqrt{-\lambda}(\eta+c)) - \sinh(2\sqrt{-\lambda}(\eta+c)) - a\}}{a + \cosh(2\sqrt{-\lambda}(\eta+c)) - \sinh(2\sqrt{-\lambda}(\eta+c))}\right\}\right]^{\frac{1}{2(\lambda k+\sqrt{\lambda^2 k^2+\lambda k})}},$$

$$E_{7,8} = \left[L_0\left\{1 + \frac{\sqrt{\lambda^2 k^2 + \lambda k}}{\lambda\sqrt{-\lambda k^2 - k}}\frac{\sqrt{-\lambda}\{a - \cosh(2\sqrt{-\lambda}(\eta+c)) - \sinh(2\sqrt{-\lambda}(\eta+c))\}}{a + \cosh(2\sqrt{-\lambda}(\eta+c)) + \sinh(2\sqrt{-\lambda}(\eta+c))}\right\}\right]^{\frac{1}{2(\lambda k+\sqrt{\lambda^2 k^2+\lambda k})}}.$$

For $\lambda > 0$,

$$E_{9,10} = \left[L_0\left\{1 + \frac{\sqrt{\lambda^2 k^2 + \lambda k}}{\lambda\sqrt{-\lambda k^2 - k}}\frac{\sqrt{(a^2-b^2)\lambda} - a\sqrt{\lambda}\,\cos(2\sqrt{\lambda}(\eta+c))}{a\sin(2\sqrt{\lambda}(\eta+c)) + b}\right\}\right]^{\frac{1}{2(\lambda k+\sqrt{\lambda^2 k^2+\lambda k})}},$$

$$E_{11,12} = \left[L_0\left\{1 + \frac{\sqrt{\lambda^2 k^2 + \lambda k}}{\lambda\sqrt{-\lambda k^2 - k}}\frac{-\sqrt{(a^2-b^2)\lambda} - a\sqrt{\lambda}\,\cos(2\sqrt{\lambda}(\eta+c))}{a\sin(2\sqrt{\lambda}(\eta+c)) + b}\right\}\right]^{\frac{1}{2(\lambda k+\sqrt{\lambda^2 k^2+\lambda k})}},$$

$$E_{13,14} = \left[L_0\left\{1 + \frac{\sqrt{\lambda^2 k^2 + \lambda k}}{\lambda\sqrt{-\lambda k^2 - k}}\frac{\sqrt{\lambda}\{i\cos(2\sqrt{\lambda}(\eta+c)) + \sin(2\sqrt{\lambda}(\eta+c)) - ia\}}{a + \cos(2\sqrt{\lambda}(\eta+c)) - i\sin(2\sqrt{\lambda}(\eta+c))}\right\}\right]^{\frac{1}{2(\lambda k+\sqrt{\lambda^2 k^2+\lambda k})}},$$

$$E_{15,16} = \left[L_0\left\{1 + \frac{\sqrt{\lambda^2 k^2 + \lambda k}}{\lambda\sqrt{-\lambda k^2 - k}}\frac{\sqrt{\lambda}\{-i\cos(2\sqrt{\lambda}(\eta+c)) + \sin(2\sqrt{\lambda}(\eta+c)) + ia\}}{a + \cos(2\sqrt{\lambda}(\eta+c)) + i\sin(2\sqrt{\lambda}(\eta+c))}\right\}\right]^{\frac{1}{2(\lambda k+\sqrt{\lambda^2 k^2+\lambda k})}}.$$

For $\lambda = 0$,

$$E_{17,\,18} = \left[\pm\frac{1}{2^{3/2}}\sqrt{\frac{r}{\ell\sqrt{-\lambda k^2-k}}}\left\{1+\frac{\sqrt{\lambda^2k^2+\lambda k}}{\lambda\sqrt{-\lambda k^2-k}}\left(-\frac{1}{\eta+c}\right)\right\}\right]^{\frac{1}{2(\lambda k+\sqrt{\lambda^2k^2+\lambda k})}},$$

where $L_0 = \pm\frac{1}{2^{3/2}}\sqrt{\frac{r}{\ell\sqrt{-\lambda k^2-k}}}$ and $\eta = \frac{x^\alpha}{\sqrt{1+\alpha}} - w\frac{t^\beta}{\sqrt{1+\beta}}$.

Set 2:

$$n = 4(\lambda k+\sqrt{\lambda^2k^2+\lambda k}),\quad w = \pm\frac{r}{2\sqrt{-\lambda k^2-k}},\quad L_0 = \pm\frac{1}{2^{3/2}}\sqrt{\frac{r}{\ell\sqrt{-\lambda k^2-k}}},$$

$$L_1 = 0,\quad M_1 = \pm\frac{1}{2^{3/2}}\sqrt{\frac{r}{\ell\sqrt{-\lambda k^2-k}}}\sqrt{\frac{\lambda^2k^2+\lambda k}{-\lambda k^2-k}}.$$

The following general results of Eq. (11) are found by using **Set 2** and combining Eqs (8), (9), (10), and (15):
For $\lambda < 0$,

$$E_{19,\,20} = \left[L_0\left\{1+\frac{\sqrt{\lambda^2k^2+\lambda k}}{\sqrt{-\lambda k^2-k}}\frac{a\sinh(2\sqrt{-\lambda}(\eta+c))+b}{\sqrt{-(a^2+b^2)\lambda}-a\sqrt{-\lambda}\cosh(2\sqrt{-\lambda}(\eta+c))}\right\}\right]^{\frac{1}{2(\lambda k+\sqrt{\lambda^2k^2+\lambda k})}},$$

$$E_{21,\,22} = \left[L_0\left\{1+\frac{\sqrt{\lambda^2k^2+\lambda k}}{\sqrt{-\lambda k^2-k}}\frac{a\sinh(2\sqrt{-\lambda}(\eta+c))+b}{-\sqrt{-(a^2+b^2)\lambda}-a\sqrt{-\lambda}\cosh(2\sqrt{-\lambda}(\eta+c))}\right\}\right]^{\frac{1}{2(\lambda k+\sqrt{\lambda^2k^2+\lambda k})}},$$

$$E_{23,\,24} = \left[L_0\left\{1+\frac{\sqrt{\lambda^2k^2+\lambda k}}{\sqrt{-\lambda k^2-k}}\frac{a+\cosh(2\sqrt{-\lambda}(\eta+c))-\sinh(2\sqrt{-\lambda}(\eta+c))}{\sqrt{-\lambda}\{\cosh(2\sqrt{-\lambda}(\eta+c))-\sinh(2\sqrt{-\lambda}(\eta+c))-a\}}\right\}\right]^{\frac{1}{2(\lambda k+\sqrt{\lambda^2k^2+\lambda k})}},$$

$$E_{25,\,26} = \left[L_0\left\{1+\frac{\sqrt{\lambda^2k^2+\lambda k}}{\sqrt{-\lambda k^2-k}}\frac{a+\cosh(2\sqrt{-\lambda}(\eta+c))+\sinh(2\sqrt{-\lambda}(\eta+c))}{\sqrt{-\lambda}\{a-\cosh(2\sqrt{-\lambda}(\eta+c))-\sinh(2\sqrt{-\lambda}(\eta+c))\}}\right\}\right]^{\frac{1}{2(\lambda k+\sqrt{\lambda^2k^2+\lambda k})}}.$$

For $\lambda > 0$,

$$E_{27,\,28} = \left[L_0\left\{1+\frac{\sqrt{\lambda^2k^2+\lambda k}}{\sqrt{-\lambda k^2-k}}\frac{a\sin(2\sqrt{\lambda}(\eta+c))+b}{\sqrt{(a^2-b^2)\lambda}-a\sqrt{\lambda}\cos(2\sqrt{\lambda}(\eta+c))}\right\}\right]^{\frac{1}{2(\lambda k+\sqrt{\lambda^2k^2+\lambda k})}},$$

$$E_{29,\,30} = \left[L_0\left\{1+\frac{\sqrt{\lambda^2k^2+\lambda k}}{\sqrt{-\lambda k^2-k}}\frac{a\sin(2\sqrt{\lambda}(\eta+c))+b}{-\sqrt{(a^2-b^2)\lambda}-a\sqrt{\lambda}\cos(2\sqrt{\lambda}(\eta+c))}\right\}\right]^{\frac{1}{2(\lambda k+\sqrt{\lambda^2k^2+\lambda k})}},$$

$$E_{31,\,32} = L_0\left[1+\frac{\sqrt{\lambda^2k^2+\lambda k}}{\sqrt{-\lambda k^2-k}}\frac{a+\cos(2\sqrt{\lambda}(\eta+c))-i\sin(2\sqrt{\lambda}(\eta+c))}{\sqrt{\lambda}\{i\cos(2\sqrt{\lambda}(\eta+c))+\sin(2\sqrt{\lambda}(\eta+c))-ia\}}\right]^{\frac{1}{2(\lambda k+\sqrt{\lambda^2k^2+\lambda k})}},$$

$$E_{33,\,34} = L_0\left[1+\frac{\sqrt{\lambda^2k^2+\lambda k}}{\sqrt{-\lambda k^2-k}}\frac{a+\cos(2\sqrt{\lambda}(\eta+c))+i\sin(2\sqrt{\lambda}(\eta+c))}{\sqrt{\lambda}\{-i\cos(2\sqrt{\lambda}(\eta+c))+\sin(2\sqrt{\lambda}(\eta+c))+ia\}}\right]^{\frac{1}{2(\lambda k+\sqrt{\lambda^2k^2+\lambda k})}}.$$

For $\lambda = 0$,

$$E_{35,\,36} = \left[\pm\frac{1}{2^{3/2}}\sqrt{\frac{r}{\ell\sqrt{-\lambda k^2-k}}}\left\{1+\frac{\sqrt{\lambda^2k^2+\lambda k}}{\sqrt{-\lambda k^2-k}}(-\eta-c)\right\}\right]^{\frac{1}{2(\lambda k+\sqrt{\lambda^2k^2+\lambda k})}},$$

where $L_0 = \pm\frac{1}{2^{3/2}}\sqrt{\frac{r}{\ell\sqrt{-\lambda k^2-k}}}$ and $\eta = \frac{x^\alpha}{\sqrt{1+\alpha}} - w\frac{t^\beta}{\sqrt{1+\beta}}$.

Set 3:

$$n = 8(2\lambda k+\sqrt{4\lambda^2k^2+\lambda k}),\quad w = \pm8\frac{\sqrt{-2\ell\lambda r\sqrt{-4\lambda k^2-k}}}{\sqrt{-4\lambda k^2-k}},$$

$$L_0 = \pm\frac{\sqrt{r\lambda}}{4\sqrt{\ell}}\frac{1}{\sqrt{-2\sqrt{-4\lambda k^2-k}}}\sqrt{\frac{-4\lambda k^2-k}{4\lambda^2k^2+\lambda k}},\quad L_1 = \pm\frac{1}{2}\frac{\sqrt{r}}{\sqrt{\ell\lambda}\sqrt{-2\sqrt{-4\lambda k^2-k}}},$$

$$M_1 = \pm\frac{1}{768}\frac{r\sqrt{r}}{k\ell\sqrt{\lambda\ell}}\frac{\sqrt{-4\lambda k^2-k}}{(4k\lambda+1)\sqrt{-2\sqrt{-4\lambda k^2-k}}}.$$

Other solutions can be written in a similar manner due to **Set 3** as well as combining Eqs (8), (9), (10), and (15). Few are as follows:

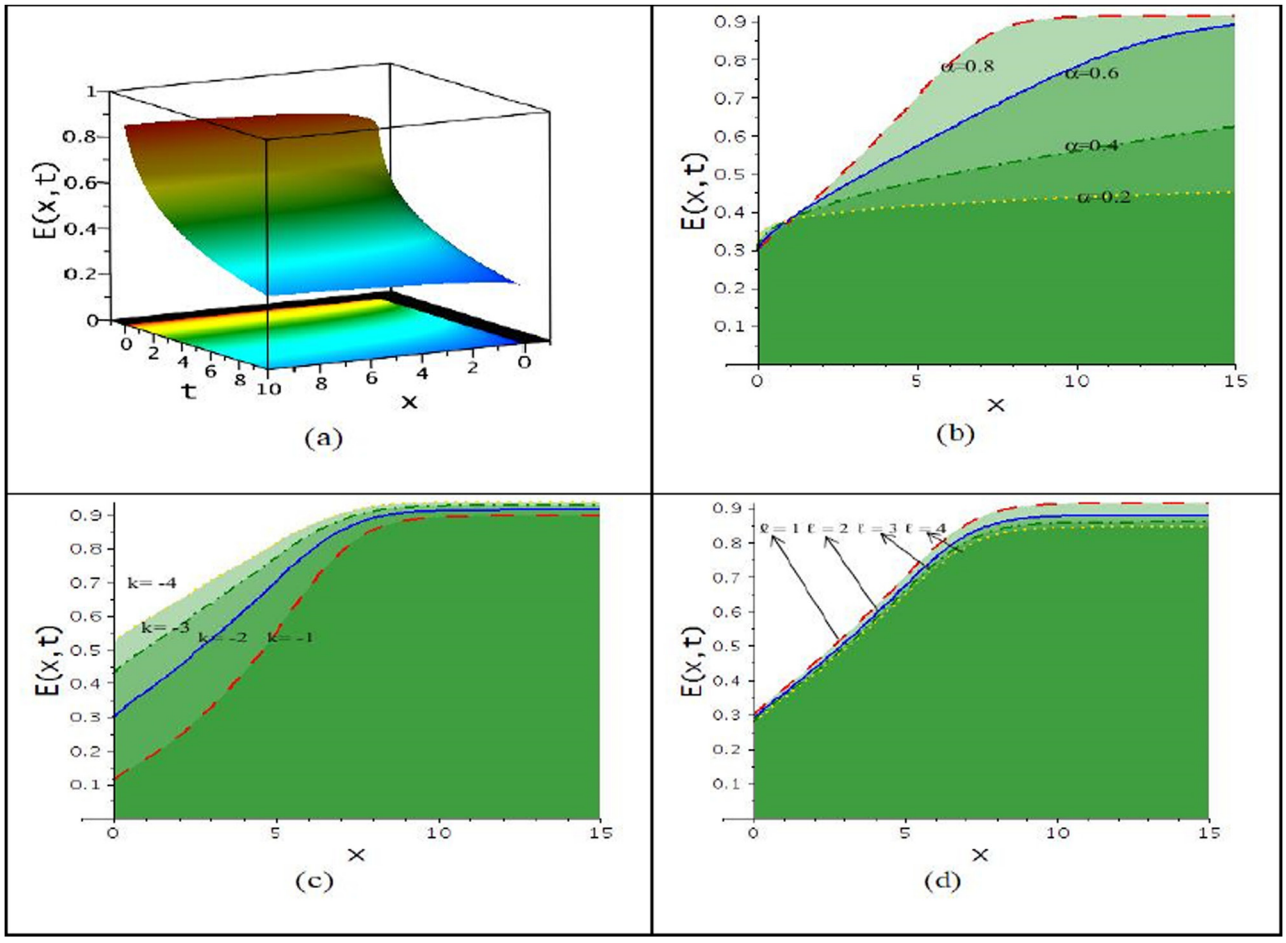

Figure 1: Shock wave solution *via* E_1: (a) 3D (upper) and contour (lower) plots, (b) effects of fractionality due to changes of α, (c) effect of dispersion due to changes of k, and (d) effects of nonlinearity.

4.2 Solutions by NFMK technique

Subsequently, due to the balance number $N = 1$, the test solution according to NFMK scheme is

$$\upsilon(\eta) = \mu_0 + \mu_1\psi(\eta), \tag{20}$$

with $\psi(\eta) = \frac{p\Theta(\eta)}{p + g(\Theta(\eta) - 1)}$; $g \neq 0$.

Differentiating Eq. (20) sufficient times and taking advantage of Eq. (11) yields a class of equations whose solutions are as follows:

$$\delta = \mp\frac{p}{\ln(a)\sqrt{2k(p+2)}}, \quad w = \pm\frac{r\sqrt{2k(p+2)}}{k(p+4)}, \quad \mu_0 = 0,$$
$$\mu_1 = \pm\frac{\sqrt{r\sqrt{2k(p+2)}}}{\sqrt{2\ell k(p+4)}}$$

and

$$\delta = \mp\frac{p}{\ln(a)\sqrt{2k(p+2)}}, \quad w = \pm\frac{2r(p+2)}{(p+4)\sqrt{2k(p+2)}},$$
$$\mu_0 = \pm\frac{\sqrt{r}}{\sqrt{\ell(p+4)k}}, \quad \mu_1 = \pm\frac{\sqrt{r}}{\sqrt{-\ell(p+4)k}}.$$

These two constraints afford new categorical wave solutions that are

$$E_{37,38} = \left\{\pm\frac{\sqrt{r\sqrt{2k(p+2)}}}{\sqrt{2\ell k(p+4)}}\frac{p}{p + c(g+1)a^{\mp\frac{p}{\ln(a)\sqrt{2k(p+2)}}\eta}}\right\}^{2/n},$$

where $\eta = \frac{kx^\alpha}{\sqrt{1+\alpha}} \mp \frac{r\sqrt{2k(p+2)}}{k(p+4)}\frac{t^\beta}{\sqrt{1+\beta}}$, and

$$E_{39,40} = \left[\pm\frac{\sqrt{r}}{\sqrt{\ell(p+4)k}}\left\{1 \pm i\frac{p}{p + c(g+1)a^{\mp\frac{p}{\ln(a)\sqrt{2k(p+2)}}\eta}}\right\}\right]^{2/n},$$

where $\eta = \frac{kx^\alpha}{\sqrt{1+\alpha}} \mp \frac{2r(p+2)}{(p+4)\sqrt{2k(p+2)}}\frac{t^\beta}{\sqrt{1+\beta}}$.

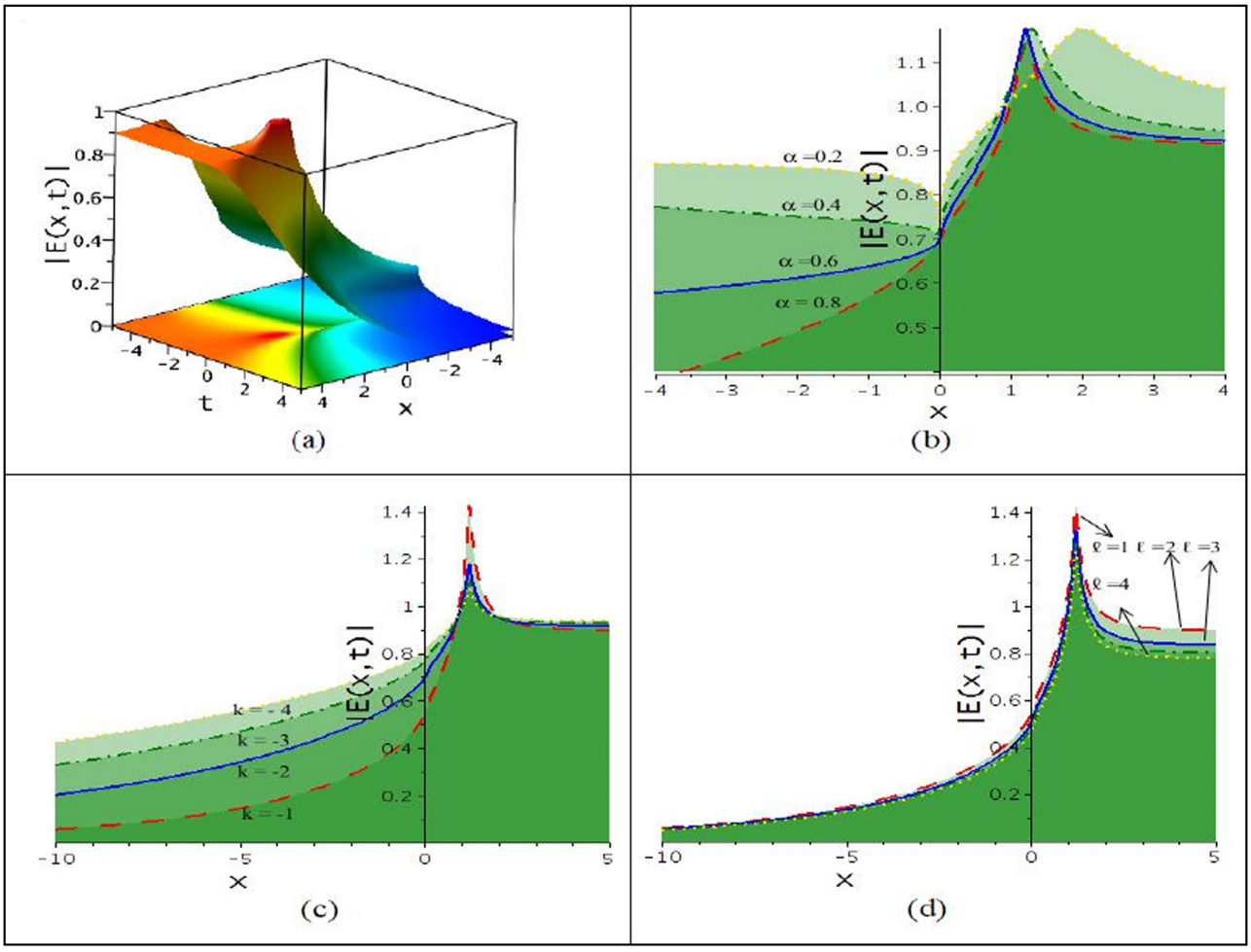

Figure 2: Modulation of shock-peaked wave solution $|E_1|$: (a) 3D (upper) and contour (lower) plots, (b) effects of fractionality due to changes of α, (c) effect of dispersion due to changes of k, and (d) effects of nonlinearity.

5 Results and discussions

This section explained the numerical representation of the obtained solution through the unified and NFMK techniques.

5.1 Numerical illustration of solutions by unified technique

All the solutions are achieved by the unified scheme in terms of trigonometric, hyperbolic, and rational functions that presented periodic, solitonic, and singular solitonic behaviors, respectively, with general parametric power nonlinearity. Actually, 54 solutions by the set of constraints are gathered here. Various distinct behaviors are illustrated with regard to particular values of free parameters in 3-D, 2-D, and contour plots. In Figure 1: shock-like wave E_1 for $\alpha = 0.8$, $\beta = 0.4$, $k = -2$, $\ell = 1$, $\lambda = -1$, $a = 1$, $b = 2$, $c = 0$, and $r = 1$, 3D and contour plots in Figure 1(a); effects of space fractionality due to changes of α are presented in Figure 1(b); effects of dispersion due to changes of k are presented in Figure 1(c); and effects of nonlinearity exhibited in Figure 1(d). But the same solution E_1 presents complexiton due to changes of parameters as $\alpha = 0.8$, $\beta = 0.4$, $k = -1$, $\ell = 1$, $\lambda = -1$, $a = 1$, $b = 2$, $c = 0$, and $r = 1$, as depicted in Figure 2; all effects of variation fractionality, dispersion, and nonlinearity parameters are illustrated in Figure 2(a–c). Due to the reduction of fractional parameters, the wave height is reduced with the wave being flat, as shown in Figures 1(b) and 2(b); the reduction of dispersion parameter effects the wave shock to reduce its hight and make the peacked flatted, Figures 1(c) and 2(c); increases in the nonlinear effect cause a slight reduction in wave height, as shown in Figures 1(d) and 2(d).

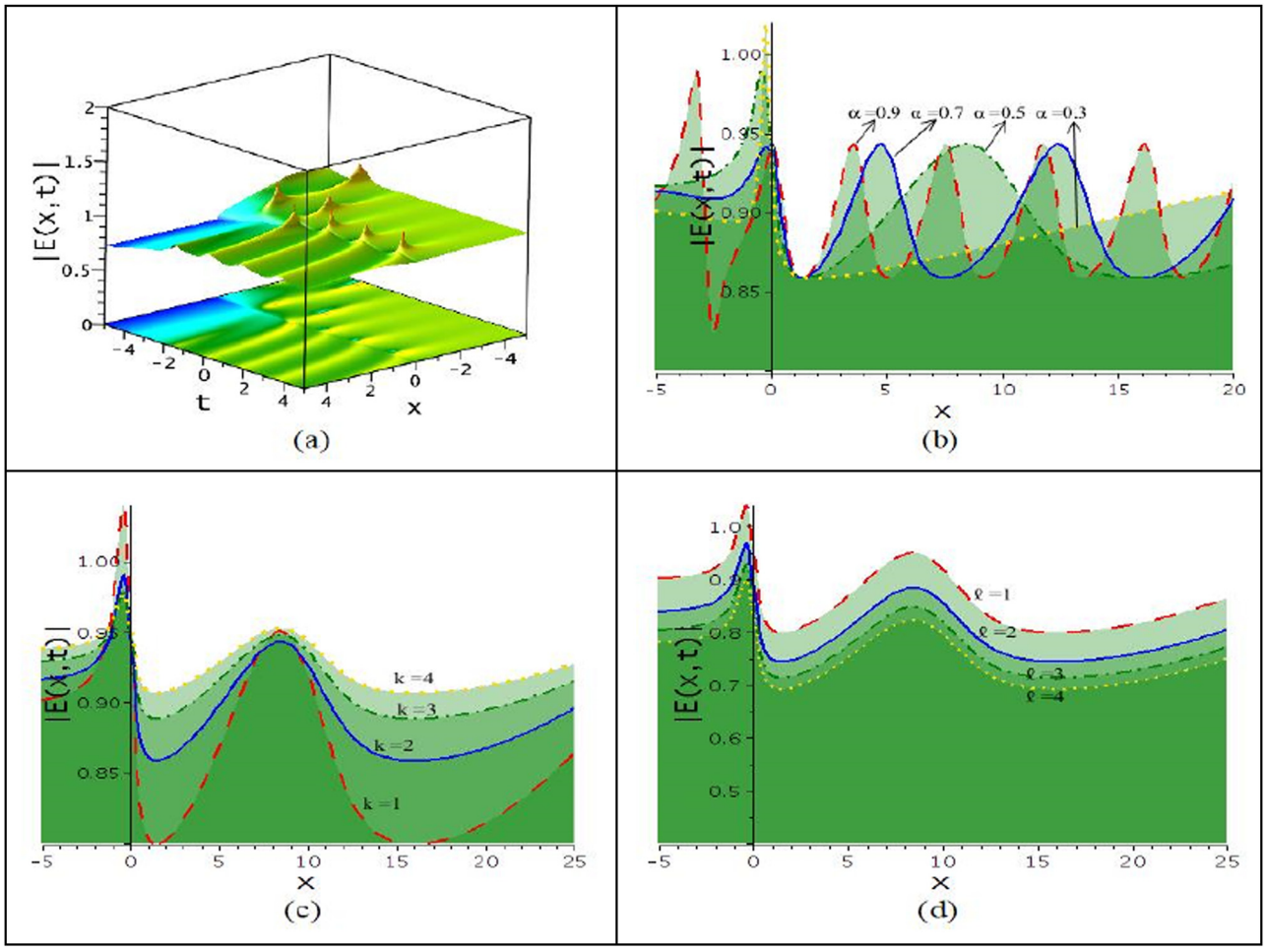

Figure 3: Modulation of periodic wave solution $|E_9|$: (a) 3D (upper) and contour (lower) plots, (b) effects of fractionality due to changes of α, (c) effect of dispersion due to changes of k, and (d) effects of nonlinearity.

In Figure 3: modulus plots of periodic wave is depicted *via* $|E_9|$ for $\alpha = 0.5$, $\beta = 0.9$, $k = 2$, $\ell = 1$, $\lambda = 1$, $a = 1$, $b = 2$, $c = 0$, and $r = 1$; effects of fractionality observed as the wave height much with wavelength small for higher values of fractional parameter, but it height reduced with increase of wave length as the fractional parameter reduced, Figure 3(b); reversed effect is observed for increasing values of dispersion, Figure 3(c); slightly change of wave height is visible in Figure 3(d) for change of nonlinearity. Figure 4, illustrated four solutions which has the similar parametric effects like above figures. Figure 4(a) shock wave E_{21} for $\alpha = 0.5$, $\beta = 0.9$, $k = 3$, $\ell = 1$, $\lambda = -1$, $a = 1$, $b = 2$, $c = 0$, $r = 1$, Figure 4(b) shock wave E_{23} for $\alpha = 0.6$, $\beta = 0.9$, $k = 3$, $\ell = 1$, $\lambda = -1$, $a = 1$, $b = 2$, $c = 0$, $r = 1$, (c) modulus plot of $|E_{27}|$ and (d) modulus plot of $|E_{33}|$ for $\alpha = 0.6$, $\beta = 0.9$, $k = 3$, $\ell = 1$, $\lambda = 1$, $a = 1$, $b = 2$, $c = 0$, $r = 1$. Figure 4(c and d) expresses periodic wave with a single shock.

In Figure 5, the modulation wave solution (from Set-3) presents dark peaked wave taking with $\beta = 0.9$, $k = 3$, $\ell = 1$, $\lambda = -1$, $a = 2$, $b = 3$, $c = 0$, $r = 1$; Figure 5(a) shows the second equation of Eq. (8) with $\alpha = 0.6$ and Figure 5(b) shows the third equation of Eq. (8) with $\alpha = 0.7$. Figure 5(c) presents a shock with a dark peak from the fourth equation of Eq. (8) for $\alpha = 0.8$, $\beta = 0.9$, $k = 0.5$, $\ell = 1$, $\lambda = -1$, $a = 2$, $b = 3$, $c = 0$, $r = 1$, and Figure 5(d) presents a periodic shock from the first equation of Eq. (9) for $\alpha = 0.5$, $\beta = 0.9$, $k = 0.5$, $\ell = 1$, $\lambda = 1$, $a = 2$, $b = 3$, $c = 0$, $r = 1$.

5.2 Numerical illustration of solutions by NFMK technique

This NFMK scheme extracted only two solutions on the basis of arbitrary parameters. Due to the change of values, it illustrated various appeals in a diverse wave pattern.

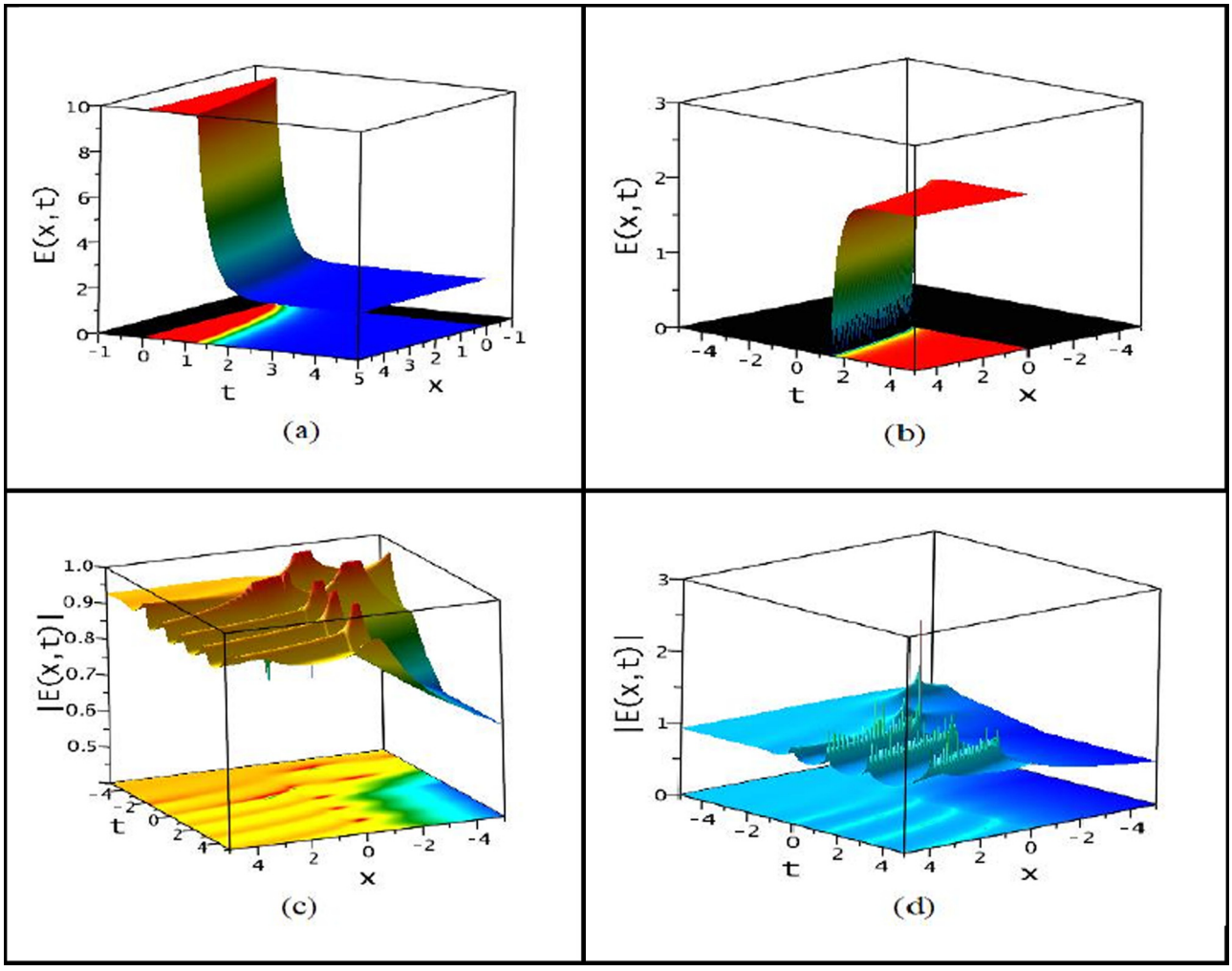

Figure 4: Wave solutions with 3D (upper) as well as contour (below) plots as (a) E_{21}, (b) E_{23}, (c) modulus plot of $|E_{27}|$, and (d) modulus plot of $|E_{33}|$.

Few are expressed with particular numerical values. The increasing and decreasing of wave height for change in parameters and fractionality are presented in Figure 6 for $\alpha = 0.5$, $\beta = 0.8$, $a = 4$, $p = 2$, $r = 0.3$, $k = -1$, $\ell = g = 1$, $n = 3$, and$c = 0.5$ and Figure 7 for $\alpha = 0.5$, $\beta = 0.8$, $a = -4$, $p = 10$, $r = 0.3$, $k = -1$, $\ell = g = 1$, $n = 3$, and $c = 0.5$.

6 Stability analysis

In this fragment, we have derived the conditions of stability of model (1) and doing so let us consider the perturbed solution

$$E = p_0 + \tau W(x,\ t), \tag{21}$$

where p_0 is a steady-state seed solution of the Eq. (1).

Applying (21) into Eq. (1), convert to the form

$$\tau w_t + \ell D_x(p_0 + \tau w)^{n+1} - r\tau w_{xx} - k\tau w_{xxt} = 0.$$

$$\Rightarrow \tau w_t + \ell(n+1)(p_0 + \tau w)^n \tau w_x - r\tau w_{xx} - k\tau w_{xxt} = 0. \tag{22}$$

Linearizing the above equation, we have

$$\tau w_t + \ell(n+1)p_0^n \tau w_x - r\tau w_{xx} - k\tau w_{xxt} = 0.$$

Again setting $w = e^{i(\rho_1 x + w_0 t)}$ into the Eq. (22) yields

$$\tau w_0 + \ell(n+1)\tau p_0^n \rho_1 - r\tau {\rho_1}^2 - k\tau {\rho_1}^2 w_0 = 0.$$

$$w_0 = \frac{\rho_1\{r\rho_1 - \ell(n+1)p_0^n\}}{(1 - k{\rho_1}^2)}, \tag{23}$$

where ρ_1 is the normalized wave number and w_0 is the dispersion relation.

The transmission relationships of Eq. (23) are observed here. The sign of w_0 describes that the result will grow rapidly or diminish as time passes. The stability of the dispersion Eq. (23) in a steady state is influenced by factors

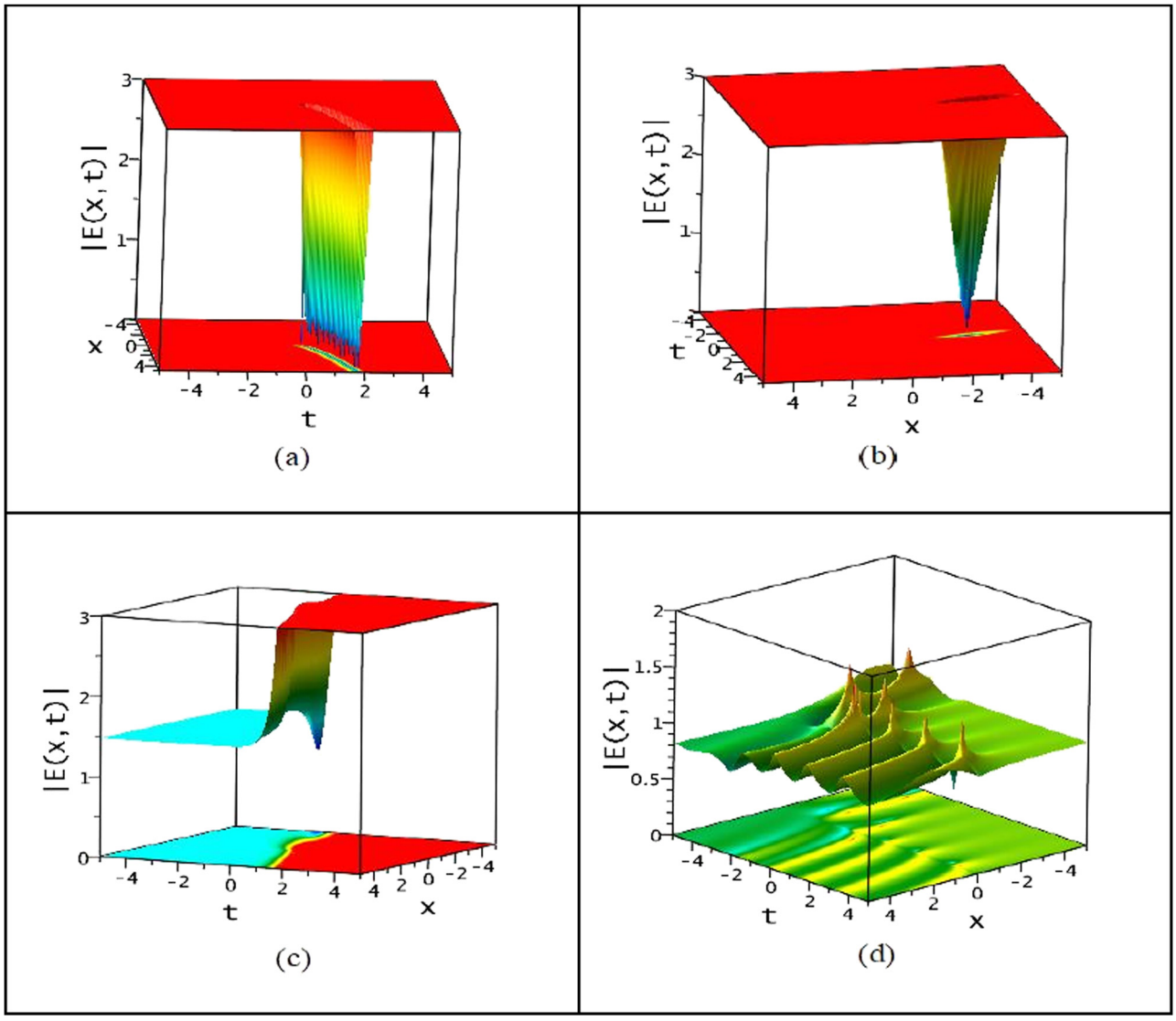

Figure 5: Modulation wave solution from **Set 3** with 3D (upper) as well as contour (below) plots: Dark peaked surf taking (a) second equation of Eq. (8) and (b) third equation of Eq. (8), (c) shock with a dark peak from fourth of Eq. (8), and (d) periodic with a shock from first equation of Eq. (9).

such as stimulated self-phase modulation, group velocity dispersion, nonlinearity and Raman scattering. The wave numbers, namely ρ_1, r, ℓ and p_0, remain stable under slight perturbations and are real when w_0 is not negative. When w_0, the wave numbers become infinite, causing the steady-state results lose stability, resulting in exponential distortion growth. Therefore, demonstrating the stability of modulation is easy to obtain for $k\rho_1^2 = 1$.

7 Comparison

In comparison with the results of [15,16], this research enriches the study of fractionality, general parametric power nonlinear solutions, and a variety of nonlinear structural wave fronts for the GEW-Burger equation. Nuruddeen and Nass [15] studied the classical and conformable fractional forms of the equation using the Kudryashov scheme, obtaining only one solution in the exponential function. Similarly, Hamdi *et al.* [16] found only one solitary wave solution for the classical GEW-Burger model, which is weaker than the result by Nuruddeen and Nass [15] (see comparison section of [15]).

In contrast, our research modifies the model in the form of Eq. (1) with the JRL fractional sense, which is considered more reliable than the conformable fractional derivative. The fractional GEW-Burger model is integrated using the unified and NFMK techniques, which encompass

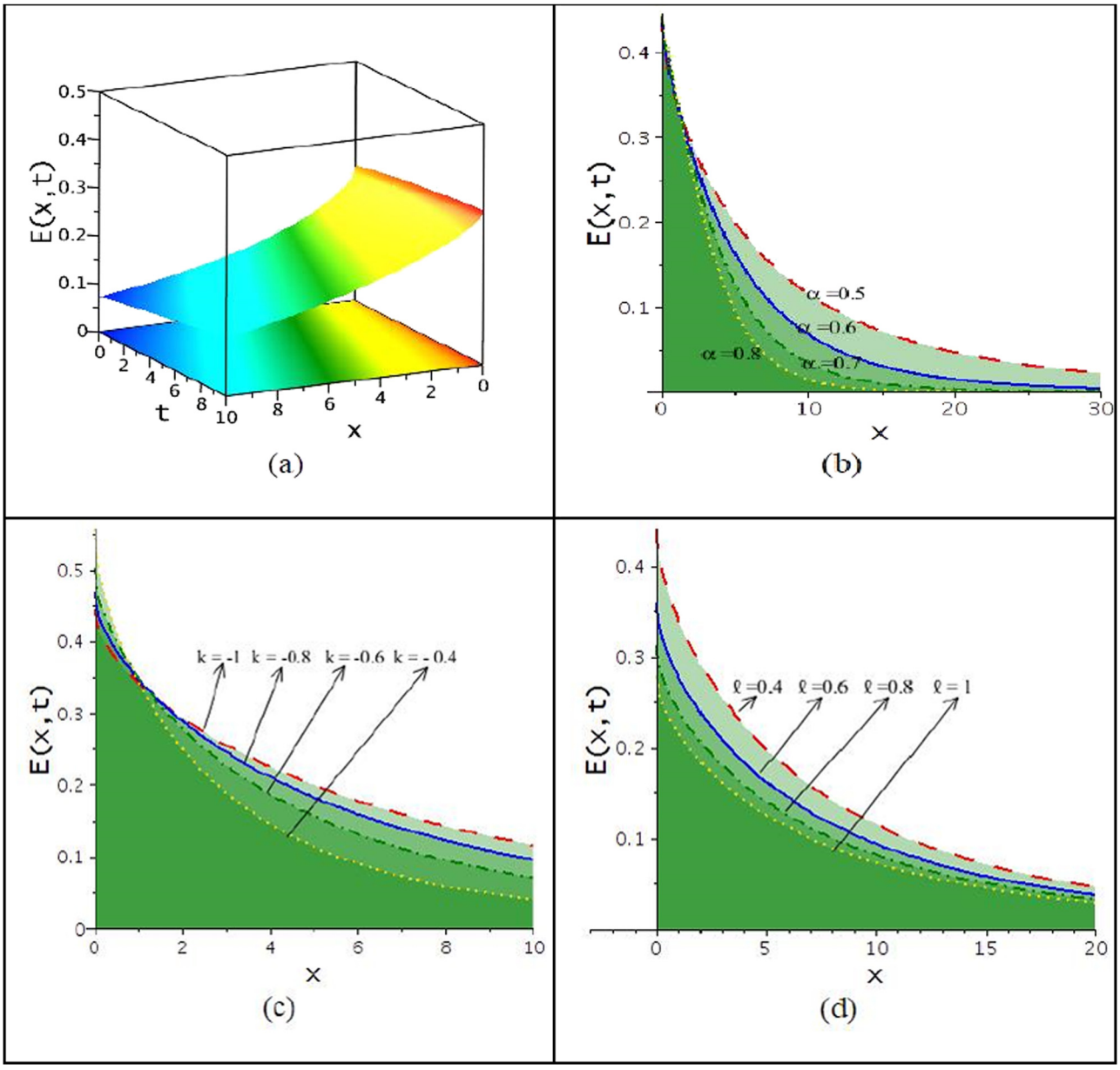

Figure 6: Modulation shock-peaked wave solution: (a) 3D (upper) and contour (lower) plots, (b) effects of fractionality due to changes of α, (c) effect of dispersion due to changes of k, and (d) effects of nonlinearity.

all solutions obtained by Nuruddeen and Nass and Hamdi *et al.* [15,16]. As a result, we achieve a vast multiplicity of solutions in terms of rational, periodic, and hyperbolic forms. Additionally, we discuss the effects of each parameter, fractionality, and general parametric power nonlinearities on the obtained results.

8 Conclusion and future works

In conclusion, this research successfully integrated the space-time JRL fractional GEW-Burgers equation using the powerful Unified and NFMK schemes. The study yielded a wide array of solutions for this model with a general parametric power nonlinearity. A comprehensive comparison was made between the results obtained in this study and those from the usual GEW-Burgers model in [15]. To aid in the comparison, 3-D graphical illustrations for specific solutions and 2-D shapes (refer to Figures 1–7) were provided, showcasing changes in nonlinearity and parameters. Furthermore, the impact of dispersion, dissipation, and general parametric power nonlinearity on wave height was observed and depicted through 3D, 2D, and contour plots (see Figures 1–7). The stability analysis is

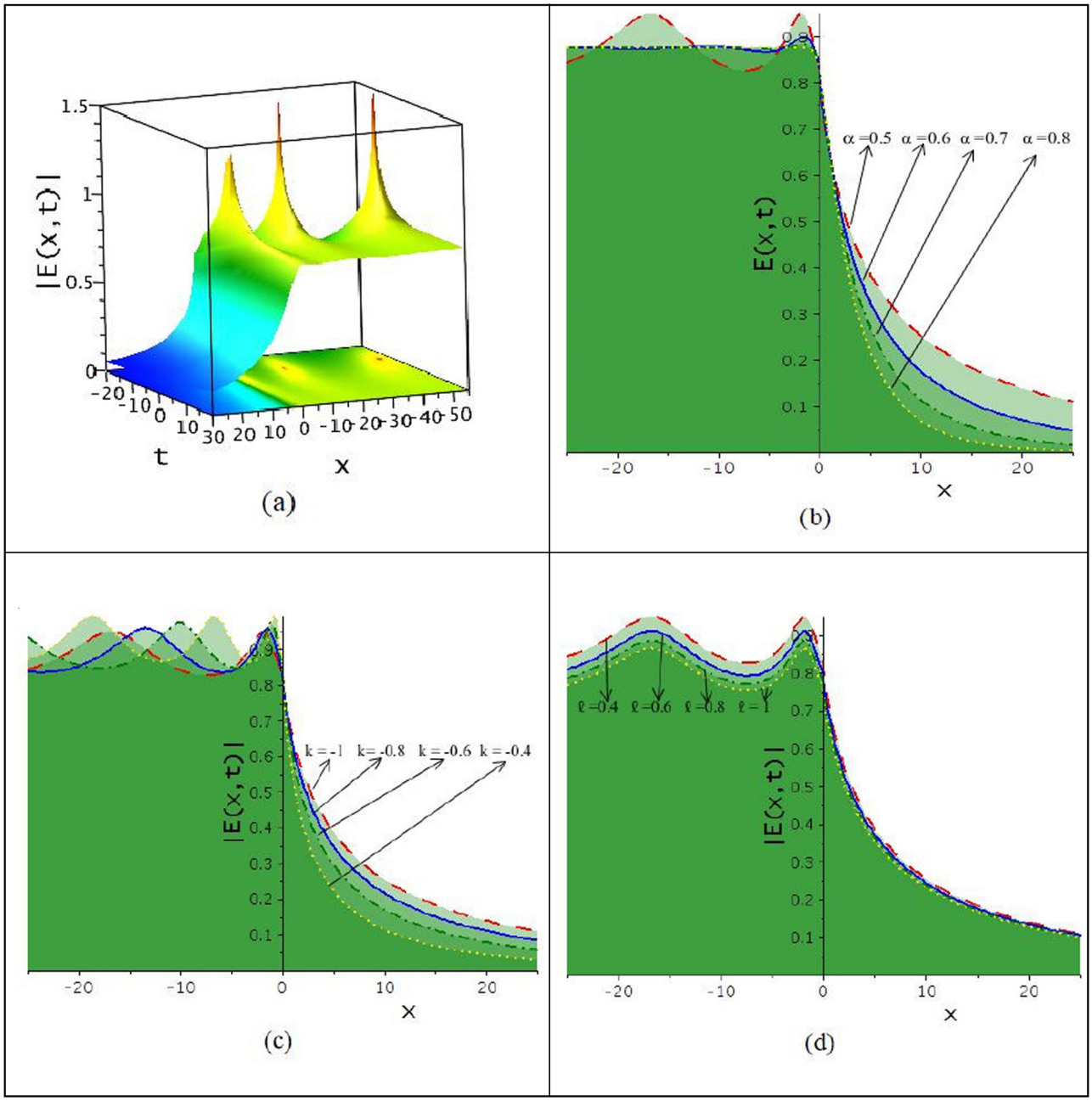

Figure 7: Modulation shock-peaked wave solution: (a) 3D (upper) and contour (lower) plots, (b) effects of fractionality due to changes of α, (c) effect of dispersion due to changes of k, and (d) effects of nonlinearity.

also performed for the considered model. The methods used in this research have several notable advantages. Firstly, they are highly versatile, enabling the discovery of solitary and periodic wave solutions with great simplicity. Secondly, exact solutions were obtained by considering various functions, making these techniques highly recommended for both general and non-general problems.

Looking ahead, our future task involves exploring the interaction of solitons, rogue waves, and bullet solitons. Additionally, the model can be further modified in M-fractional form and two-mode form to extend its applicability to different scenarios [36–39].

Acknowledgments: Thanks to the editor, reviewers, and Khalifa University, Abu Dhabi, United Arab Emirates, for technical support of the research.

Funding information: This research has external funding from Khalifa University, United Arab Emirates.

Author contributions: Methodology, software, writing – original draft, M.R. Pervin; conceptualization, software, writing – original draft, H.-O.-R.; supervision, validation, and data curation, A.A. (P. Dey); supervision, corrections and validation (S.S. Shanta); checking draft, validation, A.A. (Alrazi Abdeljabbar). All authors have read and agreed to publish this version of the manuscript.

Conflict of interest: The authors affirm that they have no known competing financial interests or personal relationships that could have seemed to influence the work reported in this paper.

Data availability statement: The manuscript has no associated data.

References

[1] Khalil R, Al Horani M, Yousef A, Sababheh M. A new definition of fractional derivative. J Comput Appl Math. 2014;264:65–70.

[2] Yang Y. The fractional residual method for solving the local fractional differential equations. Therm Sci. 2020;24(4):2535–42.

[3] Kilbas AA, Srivastava HM, Trujillo JJ. Theory and applications of fractional differential equations. North-Holland Mathematics Studies. Vol. 204. 2006.

[4] Islam Z, Abdeljabbar A, Sheikh Md, Roshid HO, Taher MA. Optical solitons to the fractional order nonlinear complex model for wave packet envelope. Results Phys. 2022;43:106095. doi: 10.1016/j.rinp.2022.106095.

[5] Abdeljabbar A, Roshid HO, Aldurayhim A. A bright, dark, and rogue wave soliton solutions of the quadratic nonlinear Klein–Gordon equation. Symmetry. 2022;14:1223. doi: 10.3390/sym14061223.

[6] Osman M, Ghanbari B. New optical solitary wave solutions of Fokas-Lenells equation in presence of perturbation terms by a novel approach. Optik. 2018;175:328–33.

[7] Guo M, Fu C, Zhang Y, Liu J, Yang H. Study of ion-acoustic solitary waves in a magnetized plasma using the three-dimensional time-space fractional Schamel-KdV equation. Complexity. 2018;2018:6852548.

[8] Jumarie G. Modified Riemann-Liouville derivative and fractional Taylor series of non-differentiable functions further results. Comput Math Appl. 2006;51:1367–76.

[9] Jumarie G. Table of some basic fractional calculus formulae derived from a modified Riemann-Liouville derivative for non-differentiable functions. Appl Math Lett. 2009;22:378–85.

[10] Nisar KS, Akinyemi L, Inc M, Şenol M, Mirzazadeh M, Houwe A, et al. New perturbed conformable Boussinesq-like equation: Soliton and other solutions. Results Phys. 2022;33:105200.

[11] Eslami M, Rezazadeh H. The first integral method for Wu–Zhang system with conformable time-fractional derivative. Calcolo. 2015;53:475.

[12] Hosseini K, Kaur L, Mirzazadeh M, Baskonus HM. 1-soliton solutions of the (2 + 1)-dimensional Heisenberg ferromagnetic spin chain model with the beta time derivative. Opt Quant Electron. 2021;53:125.

[13] Rahman Z, Abdeljabbar A, Roshid HO, Ali MZ. Novel precise solitary wave solutions of two time fractional nonlinear evolution models via the MSE scheme. Fractal Fract. 2022;6:444. doi: 10.3390/fractalfract6080444.

[14] Rahman Z, Ali MZ, Roshid HO. Closed form soliton solutions of three nonlinear fractional models through a proposed Improved Kudryashov method. Chin Phys B. 2021;30:050202.

[15] Nuruddeen RI, Nass MA. Exact solitary wave solution for the fractional and classical GEW-Burgers equations: an application of Kudryashov method. J Taibah Univ Sci. 2018;12(3):309–14. doi: 10.1080/16583655.2018.1469283.

[16] Hamdi S, Enright WH, Schiesser WE, Gottlieb JJ. Exact solutions of the generalized equal width equation. Comp Sci Appl. 2003;2668:725–34.

[17] Yusuf A, Sulaiman T, Abdeljabbar A, Alquran M. Breather waves, analytical solutions and conservation laws using Lie–Bäcklund symmetries to the (2 + 1)-dimensional Chaffee–Infante equation. J Ocean Eng Sci. 2023;8(2):145–51. doi: 10.1016/j.joes.2021.12.008.

[18] Sulaiman T, Yusuf A, Abdeljabbar A, Alquran M. Dynamics of lump collision phenomena to the (3 + 1)-dimensional nonlinear evolution equation. J Geom Phys. 2021;169:104347.

[19] Ullah MS, Ali MZ, Roshid HO, Seadawy AR, Baleanu D. Collision phenomena among lump, periodic and soliton solutions to a (2 + 1)-dimensional Bogoyavlenskii's breaking soliton model. Phys Lett A. 2021;397:127263.

[20] Ullah MS, Roshid HO, Ma WX, Ali MZ, Rahman Z. Interaction phenomena among lump, periodic and kink wave solutions to a (3 + 1)-dimensional Sharma-Tasso-Olver-like equation. Chin J Phys. 2020;68:699–711.

[21] Abdeljabbar A, Hossen MB, Roshid HO, Aldurayhim A. Interactions of rogue and solitary wave solutions to the (2 + 1)-D generalized Camassa–Holm–KP equation. Nonlinear Dyn. 2022;110:3671–83. doi: 10.1007/s11071-022-07792-x.

[22] Gomeg CS, Roshid HO, Inc M, Akinyemi L, Rezazadeh H. On soliton solutions for perturbed Fokas-Lenells equation. Opt Quantum Electron. 2022;54:307.

[23] Hoque MF, Roshid HO. Optical soliton solutions of the Biswas-Arshed model by the tanh expansion approach. Phys Scr. 2020;95:075219.

[24] Akram G, Sadaf M, Khan MAU. Abundant optical solitons for Lakshmanan-Porsezian-Daniel model by the modified auxiliary equation method. Optik. 2022;251:168163.

[25] Kumar A, Arora R. Soliton solution for the BBM and MRLW equations by cosine-function method. Optim Comput. 2011;49:59–61.

[26] Kumar A, Arora R. Solutions of the coupled system of Burgers equations and coupled Klein-Gordon equation by RDT method. Int J Adv Math Mech. 2013;1(2):103–15.

[27] Ismael HF, Murad MAS, Bulut H. M-lump waves and their interaction with multi-soliton solutions for a generalized Kadomtsev-Petviashvili equation in (3 + 1)-dimensions. Chin J Phys. 2022;77:1357–64.

[28] Gaillard P. Rational solutions to the KPI equation from particular polynomials. Wave Motion. 2022;108:102828.

[29] Rao J, Chow KW, Mihalache D, He J. Completely resonant collision of lumps and line solitons in the Kadomtsev–Petviashvili I equation. Stud Appl Math. 2021;147(3):1007–35.

[30] Guo L, Chabchoub A, He J. Higher-order rogue wave solutions to the Kadomtsev-Petviashvili 1 equation. Phys D Nonlinear Phenom. 2021;426:132990.

[31] Dubrovsky VG, Topovsky AV. Multi-lump solutions of KP equation with integrable boundary via ∂-dressing method. Phys D Nonlinear Phenom. 2020;414:132740.

[32] Gözükızıl OF, Akcagil S, Aydemir T. Unification of all hyperbolic tangent function methods. Open Phys. 2016;14:524–41.
[33] Akcagil S, Aydemir T. A new application of the unified method. New Trends Math Sci. 2018;6(1):185–99.
[34] Ullah MS, Roshid HO, Ali MZ, Biswas A, Ekici M, Khan S, et al. Optical soliton polarization with Lakshmanan-Porsezian-Daniel model by unified approach. Results Phys. 2021;22:103958.
[35] Ali KK, Mehanna MS, Abdel-Aty AH, Wazwaz AM. New soliton solutions of Dual mode Sawada Kotera equation using a new form of modified Kudryashov method and the finite difference method. J Ocean Eng Sci. 2022. doi: 10.1016/j.joes.2022.04.033.
[36] Wang J, Shehzad K, Seadawy AR, Arshad M, Asmat F. Dynamic study of multi-peak solitons and other wave solutions of new coupled KdV and new coupled Zakharov–Kuznetsov systems with their stability. J Taibah Univ Sci. 2023;17(1):2163872.
[37] Seadawy AR, Cheemaa N. Some new families of spiky solitary waves of one-dimensional higher-order K-dV equation with power law nonlinearity in plasma physics. Indian J Phys. 2020;94:117–26.
[38] Younas U, Seadawy AR, Younis M, Rizvi STR. Optical solitons and closed form solutions to the (3 + 1)-dimensional resonant Schrödinger dynamical wave equation. Int J Mod Phys B. 2020;34(30):2050291.
[39] Khan N, Ahmad Z, Shah J, Murtaza S, Albalwi MD, Ahmad H, et al. Dynamics of chaotic system based on circuit design with Ulam stability through fractal-fractional derivative with power law kernel. Sci Rep. 2023;13:5043.